euspen's 24th International Conference & Exhibition, Dublin, IE, June 2024
www.euspen.eu

Data-driven modeling for the correlation of the inputs and outputs in thermoplastic micro injection molding

Alireza Mollaei Ardestani[1]*, Reza Asadi[2], Uma Maheshwaran Radhakrishnan[1], Inigo Flores Ituarte[2], Murat Kulahci[3], Matteo Calaon[1], Jesper Henri Hatel[1], Guido Tosello[1]

[1]Department of Civil and Mechanical Engineering, Technical University of Denmark, 2800 Kgs. Lyngby, Denmark; almoa@dtu.dk ; guto@dtu.dk
[2]Faculty of Engineering and Natural Sciences, Tampere University, Korkeakoulunkatu 6, 33014, Tampere, Finland
[3]Department of Applied Mathematics and Computer Science, Technical University of Denmark, 2800 Kgs. Lyngby, Denmark

* Corresponding author: almoa@dtu.dk

Abstract

This paper explores the application of micro manufacturing in the production of plastic parts, focusing on the widely used injection molding process. The increasing demand for high-quality parts in industrial settings has led to a heightened need for digital twins in micro injection molding. To address this demand, a Data-Driven approach is employed, involving the simulation of process parameters effects in plastic injection molding. The project employs the Design of Experiment (DOE) methodology for a specific geometry, varying three key input process parameters—Melt Temperature, Mold Temperature, and Injection Speed—across different material grades. Responses such as Part Weight, Cavity Injection Time, and Maximum Injection Pressure are simulated using a commercially available Finite Element Analysis (FEA) Simulation software. Data Driven Modelling is achieved by incorporating viscosity and pvT coefficients of each material, along with the specified process parameters. Statistical Analysis, Machine Learning, and Deep Learning methods are employed for the data driven modeling. The results indicate that Part Weight and Maximum Injection Pressure are influenced by all three input parameters, while Cavity Injection Time is primarily affected by the Injection Speed of the machine. Both Statistical and artificial intelligence models demonstrate effective performance with the selected materials. Importantly, these models successfully predict results for materials not initially considered, affirming the achievement of Data Driven Modelling for the specific geometry under investigation.

Keywords: plastic injection molding; design of experiments; machine learning; digital twin; process optimization

1. Introduction

In the modern engineering world, the widespread adoption of algorithms has lead to a transformative era by eliminating additional costs associated with time-consuming and expensive tests in the product design and production development cycle. Contemporary modeling, prediction, and optimization methods have markedly diminished the reliance on traditional experimental trials and measurements for enhancing both product and process. This spectrum of techniques including statistical methods (such as ANOVA), machine learning methods (including artificial neural networks – ANNs), and optimization methods utilizing meta-heuristic algorithms.

In the present context, the integration of Finite Element Analysis (FEA) methods with modern optimization approaches has proven to be effective for manufacturers in identifying optimal levels of input parameters, leading to the production of products of the highest quality. Given the intricate behavior of polymers, especially during injection molding processes, the multitude of parameters influencing product quality underscores the importance of monitoring and controlling each parameter and their interactions. This becomes imperative in the prevention of injection defects.

Many studies have been conducted till now focusing on the application of data analysis in plastic injection molding process. They have used experimental tests and statistical analysis to rank the significance of some process parameters on the quality measures of the product [1,2]. In some other studies, researchers used ML-based techniques on experimental data to create a prediction model for an injection process [3,4,5]. Silva et al. [6] introduced an intelligent method to classify the quality of products. For this purpose, they employed artificial neural networks (ANNs) and support vector machines (SVMs) and a combination of the two methods. The trained models showed a good capability to predict the defects and classify them by type.

Deep Neural Networks (DNNs) are preferred over traditional Artificial Neural Networks (ANNs) due to their increased depth, signifying the presence of multiple hidden layers. This depth allows DNNs to automatically learn hierarchical representations of features, making them highly effective in handling complex tasks such as image processing [7] and other intricate problem domains. The added depth enables DNNs to capture and understand intricate patterns in injection molding data, leading to superior performance compared to shallower networks with fewer layers.

2. Materials and methods

The part under study has a dogbone-shaped geometry with the dimensions of 12×3×1 mm. the total volume of the part is 76.4 mm^3, and the surface of the part is 241.2 mm^2. The mould has 2 cavities (see Figure 1). For this study, 36 different grades of different classes of thermoplastic polymers (both amorphous and semi-crystalline) have been chosen. The list includes ABS (Terluran EGP-7, Novodur E211, ALCOM AWL 10WT 1308-05 LB, Terluran 2802 TR, Terluran GP 22, Sinkral F332), COPE (Tritan MX731, Eastar DN011), HDPE (Dowlex IP60), PA6 (Ultrmid B3K), PA12 (Grilamid L20L), PC (Iupilon S-2000), PES (Ultrason E2010G6), PET (Petro 140), PMMA (95UX-BK 13, Altuglas drm), POM (Ultraform N2640 E2, Ultraform N2320 003, Ultraform S2320 003), PP (80CM-NC 601, ALCOM PP 6201 WT 0134-05LB, Exxon Mobil PP1013H1), PS (Polystyrol 456M), SAN (Kostil B266), PLA (Natureworks 7000D), PEEK (RTP 2205HF), PBT (Ultradur B4500), PVC (Polyvin 6620), LDPE (Lacqtene 1003 FL 22), PPO (Noryl 731), PPSU (Ultrason P 3010), PEI (Ultem 1000), PSU (Ultrason S 2010), PPS (Fortron 1131L4), LCP (Vectra A430), and PAI (Torlon 5030). In the beginning, the CAD geometry of the part was created. Then the model was transferred to the FEA software, Moldex 3D.

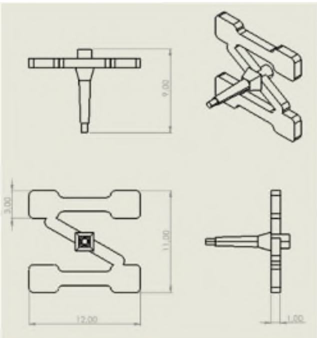

Figure 1. Micro part geometry and dimensions including miniaturized sprue, runners, and gates.

A 3D mesh with the seeding size of 0.2 mm was employed which created 12061 elements on the part. Then, for some materials, a 2-level (with the levels of -1 and +1) and for some others, a 3-level full factorial DOE (with the levels of -1, 0, +1) was employed for the 3 input factors. So, in total, 8 and 27 experiments were designed respectively. The amounts for each input variable (melt temperature, mold temperature, and injection speed) were normalized so that process parameters variations could be computed evenly across all DOEs for all the materials grades. After setting all the experiments in the FEA software, the results (part weight, cavity injection time, maximum injection pressure) were simulated and collected.

Studying and optimizing various parameters in the injection molding process is possible but time-consuming and expensive. To reduce defects, focusing on key parameters such as melt temperature, mold temperature, and injection speed is crucial. The objectives of this study considered to be the part weight, maximum injection pressure, and cavity injection time. Correlating controllable input parameters (melt temperature, mold temperature, injection speed) with output parameters (part weight, cavity injection time, maximum injection pressure) helps in implementing Data Driven Modelling in injection molding.

Every thermoplastic has specific coefficients which represent the materials properties in their respective material models. These coefficients remain constant for every selected material grade, resulting in 36 recorded levels for the corresponding 36 material grades. In this study, viscosity and pvT model coefficients of the materials are extracted from the Moldex3D material database. The list of coefficients can be seen in Table 1. After performing the simulations based on the DOE plan, all the simulated results were collected. Then, Analysis of Variance was applied on the results to provide main effect diagrams of the variables on the results. Finally, a Deep Learning (DL) algorithm was trained based on the input data to allow predictions of the process results.

Table 1 List of coefficients.

Viscosity coefficients		**pvT coefficients**	
Cross model 2	**Cross model 3**		
n	n	b1L [cc/g]	b1S [cc/g]
τ* [dyne/cm^3]	τ* [dyne/cm^3]	b2L [cc/g.K]	b2S [cc/g.K]
B [g/cm.sec]	D1 [g/cm.sec]	b3L [dyne/cm^2]	b3S [dyne/cm^2]
Tb [K]	D2 [K]	b4L[1/K]	b4S [1/K]
D [cm^2/dyne]	D3[cm^2/dyne]	b5 [K]	b6 [cm'^{2}.K/dyne]
	A1	b7 [cc/g]	b8 [1/K]
	A2b[K]	b9 [cm^2/dyne]	

In this study, two DNNs for the considered material types are provided. Figure 2 illustrates the schematic view of the proposed networks. The DNNs contain 6 hidden layers, which are fully connected to the previous and next layers without any dropout layers. For cross model (2) and cross model (3), 4 and 7 parameters are considered as viscosity parameters respectively and 13 parameters as PVT parameters. Three parameters are considered as uncontrollable parameters. In Table 2, the optimal parameters of the proposed DNN's can be observed.

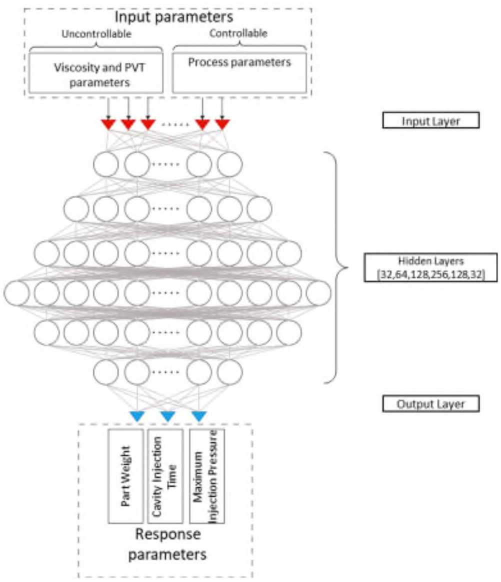

Figure 2. The DNNs architecture considered for the study.

Table 2 DNNs characteristics for Cross model 2 and 3 materials

	Cross model 2	**Cross model 3**
Number of hidden layers	6	6
Number of neurons in each layer	[32,64,128,256,128, 32]	[32,64,128,256,128, 32]
Loss function	Mean Square Error (MSE) loss	Mean Square Error (MSE) loss
Optimizer	AdamW	AdamW
Activation function of each layer	[GELU, GELU, GELU, GELU, GELU, LeakyReLU]	[ReLU6, ReLU6, ReLU6, ReLU6, ReLU6, LeakyReLU]
Starting learning rate	0.0005	0.0003
Training and validation instances	232	332

3. Results

The results of simulations were analyzed using the ANOVA method. The main effect plots for all the outputs and interaction plots for the part weight can be observed in Figure 3.

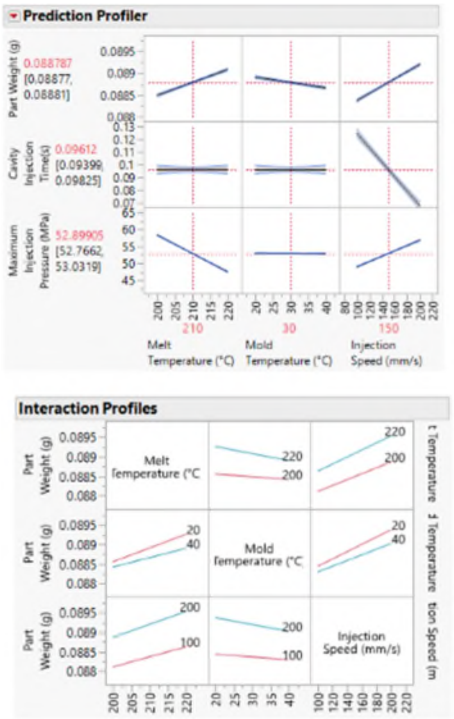

Figure 3. Main effect and interaction plots.

The interaction profiles have also been obtained for the other two output objectives, namely Cavity Injection Time and Maximum Injection Pressure. The main effect summary and the interaction effect summary of the part weight can be seen in the Figure 4. The same responses can also be provided for Cavity injection time and Maximum injection pressure.

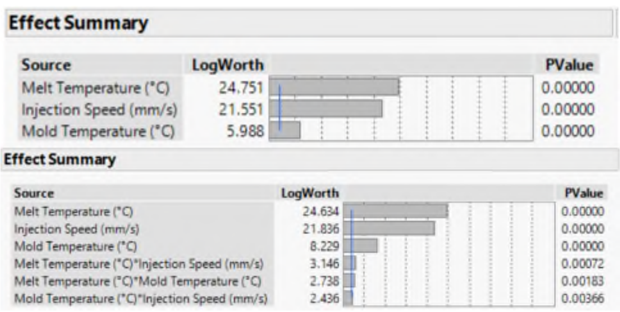

Effect Summary

Source	LogWorth	PValue
Melt Temperature (°C)	24.751	0.00000
Injection Speed (mm/s)	21.551	0.00000
Mold Temperature (°C)	5.988	0.00000

Effect Summary

Source	LogWorth	PValue
Melt Temperature (°C)	24.634	0.00000
Injection Speed (mm/s)	21.836	0.00000
Mold Temperature (°C)	8.229	0.00000
Melt Temperature (°C)*Injection Speed (mm/s)	3.146	0.00072
Melt Temperature (°C)*Mold Temperature (°C)	2.738	0.00183
Mold Temperature (°C)*Injection Speed (mm/s)	2.436	0.00366

Figure 4. Part weignt main effect and interaction summary

As a result of ANOVA, prediction regression models can be obtained. The general form of these models are as follows:

M[g] = $\mu+\beta1*(A)+\beta2*(B)+\beta3*(C)+\beta4*(A*B)+\beta5*(A*C)+\beta6*(B*C)$ (4.1)

T[s] = $\mu+\beta1*(A)+\beta2*(B)+\beta3*(C)+\beta4*(A*B)+\beta5*(A*C)+\beta6*(B*C)$ (4.2)

P[MPa] = $\mu+\beta1*(A)+\beta2*(B)+\beta3*(C)+\beta4*(A*B)+\beta5*(A*C)+\beta6*(B*C)$ (4.3)

The terms of M, T, and P are representing Part weight, Cavity injection time, and Maximum injection pressure, respectively.

The factors are interpreted as:

- A - Melt Temperature
- B - Mold Temperature
- C - Injection Speed
- AB - Melt and Mold Temperature Interaction
- AC - Melt Temperature and Injection speed Interaction
- BC - Mold Temperature and Injection speed Interaction

β1, β2, β3, β4, β5, β6 are the coefficients of the above-mentioned factors. In the equations above, μ is the mean of responses. For each material grade, all the coefficients were extracted. Since 36 materials were chosen to be investigated, 108 equations to predict the 3 outputs for each material have been extracted. The prediction results of each model are shown in Figure 7.

3.1 DNN model

In Figure 6., the training and validation outcomes of the suggested DNNs for Cross Model (2) and Cross Model (3) are depicted. The red-highlighted area signifies the occurrence of overtraining, prompting the cessation of the training process and the preservation and utilization of optimal coefficients at that point.

Table 3 provides an assessment of the performance of the trained DNNs concerning the loss functions or MSE, and RMSE. Notably, the MSE and RMSE values for Cross Model (2) exhibit a lower magnitude compared to Cross Model (3) across both training and validation datasets. However, it is noteworthy that both sets of values, specifically less than 0.0055 for MSE and 0.075 for RMSE, fall within a range deemed acceptable in the context of the given analysis.

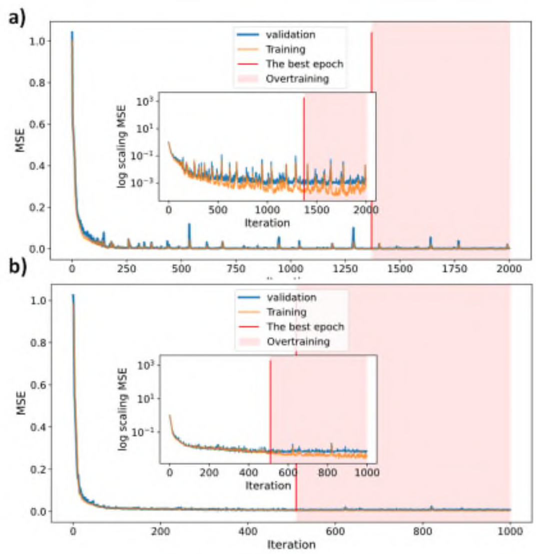

Figure 5. Training and validation loss plots of the modeling performance of a) Cross Model (2) and b) Cross Model (3), including optimal validation epochs and overtraining ranges.

Table 3. Training and validation MSE/RMSE for Cross Model (2) and Cross Model (3)

Model	Training		Validation	
	MSE	RMSE	MSE	RMSE
Cross model (2)	0.00024	0.01547	0.00060	0.02441
Cross model (3)	0.00518	0.07199	0.00538	0.07334

Following the completion of training and validation phases, the testing process is essential. The recommended method involves plotting the fit line between model output (predicted values) and target values (ground truth data). Figure 6 illustrates the fit line alongside the line y=x, depicting optimal results with an R^2 value of 1. Notably, the fitted lines for all process responses exhibit R^2 values exceeding 0.96, with slope values within the range of 0.965 and 1.093, and intercepts below 0.186. These results affirm the efficacy of the training and validation processes, showcasing the model's accuracy in predicting outcomes.

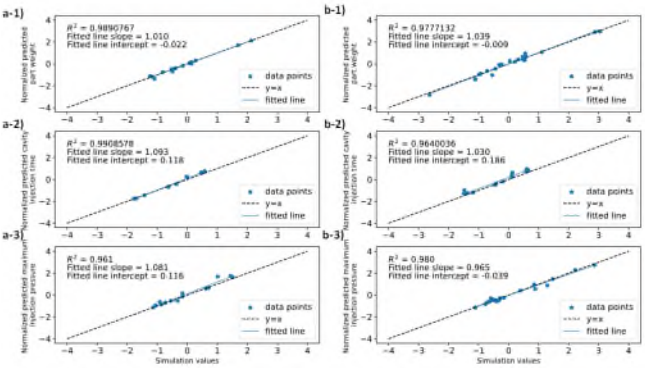

Figure 6. Testing fit lines of DNN models for 1) normalized part weight, 2) normalized cavity injection time, and 3) normalized maximum injection pressure, alongside their comparison with the identity line y=x

In the final analysis, Figure 7 offers a comprehensive comparison between the ground truth values and the predicted values generated by DNNs for Cross Model (2) and Cross Model (3) and predictions made by RSM. Notably, with only minor discrepancies observed in a few instances, where testing data exhibits trivial differences from the ground truth, the networks consistently demonstrate accurate predictions of the trends and values associated with the proposed response parameters.

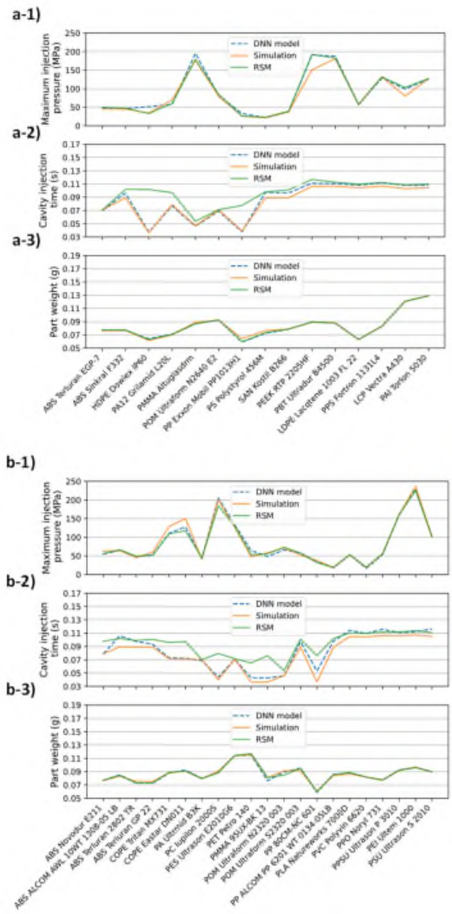

Figure 7. Comparative analysis of ground truth and predicted values by trained DNNs for a) Cross Model (2) and b) Cross Model (3), utilizing testing data alongside predictions made by RSM.

4. Conclusion

This study focused on the investigation of the effect of melt temperature, mold temperature, and injection speed on 3 part quality factors (part weight, maximum injection pressure, injection time). 36 different thermoplastic materials were studied. After performing full factorial DOEs with all materials, two types of models were assembled (based on the materials' specifications). Then, FEA was conducted, and the results were measured. Then a prediction model for each of the outputs of the process for all the 36 materials were extracted (108 in total). To investigate if we can reach higher accuracy prediction models rather than RSM models, a DNN was optimized and trained for each model. At the end, the results of RSM models' predictions were compared to those of the DNN models.

It was observed that the DNN model can predict the results with much higher accuracy compared to RSM model. The prediction accuracy of DNN for part weight, cavity injection time, and maximum injection pressure is 98.9%, 99.1%, and 96.1% for cross model 2 and 97.8%, 96.4%, and 98.0% for cross model 3.

Acknowledgements

This research work was undertaken in the context of DIGIMAN4.0 project ("DIGItal MANufacturing Technologies for Zero-defect Industry 4.0 Production", (http://www.digiman4-0.mek.dtu.dk/). DIGIMAN4.0 is a European Training Network supported by Horizon 2020, the EU Framework Programme for Research and Innovation (Project ID: 814225).

This research has been partially supported by the project Multi-disciplinary Digital Design and Manufacturing, D2M (Project ID: 346874) Research Council of Finland/Academy Research Fellow.

References

[1] Li, Y., Chen, J. C., & Ali, W. M. (2021). Process optimization and in-mold sensing enabled dimensional prediction for high precision injection molding. Int. J. on Interactive Design and Manufacturing (IJIDeM), 1-17.

[2] Asadi, R., Niknam, S. A., Anahid, M. J., Ituarte, I. F. (2023). The use of wavelet transform to evaluate the sensitivity of acoustic emission signals attributes to variation of cutting parameters in milling aluminum alloys. Int. J. of Advanced Manufacturing Technology, 126(7-8), 3039-3052.

[3] Mollaei Ardestani, A., Azamirad, G., Shokrollahi, Y., Calaon, M., Hattel, J. H., Kulahci, M., Tosello, G. (2023). Application of Machine Learning for Prediction and Process Optimization—Case Study of Blush Defect in Plastic Injection Molding. Applied Sciences, 13(4), 2617.

[4] Chen, J. C., Guo, G., & Wang, W. N. (2020). Artificial neural network-based online defect detection system with in-mold temperature and pressure sensors for high precision injection molding. International Journal of Advanced Manufacturing Technology, 110, 2023-2033.

[5] Asadi, R., Queguineur, A., Ylä-Autio, A., Martikkala, A., Wiikinkoski, O., Mokhtarian, H., Ituarte, I. F. (2023, December). Using artificial neural networks to model single bead geometries processed by laser-wire direct energy deposition. In IOP Conference Series: Materials Science and Engineering (Vol. 1296, No. 1, p. 012005). IOP Publishing.

[6] Silva, B., Sousa, J., & Alenya, G. (2021, December). Machine learning methods for quality prediction in thermoplastics injection molding. 2021 IEEE Int. Conf. on Electrical, Computer and Energy Tech., pp. 1-6.

[7] Asadi, R., Queguineur, A., Wiikinkoski, O., Mokhtarian, H., Aihkisalo, T., Revuelta, A., Ituarte, I. F. (2024). Process monitoring by deep neural networks in directed energy deposition: CNN-based detection, segmentation, and statistical analysis of melt pools. Robotics and Computer-Integrated Manufacturing, 87, 102710.